NON-LINEAR MEMS ELECTROSTATIC KINETIC ENERGY HARVESTER WITH A TUNABLE MULTISTABLE POTENTIAL FOR STOCHASTIC VIBRATIONS

F. Cottone[1], P. Basset[1], R. Guillemet[1], D. Galayko[2], F. Marty[1] and T. Bourouina[1]
[1]Université Paris-Est / ESYCOM / ESIEE Paris, France
[2]UPMC-Sorbonne Universités / LIP6 – France

ABSTRACT

We report on the first electrostatic Vibration Energy Harvester (e-VEH) using a voltage-controlled multi-stable energy potential in order to harvest energy from stochastic vibration noise. We show that an optimized pre-charge voltage on the electromechanical transducer associated with a displacement constraint of the movable mass leads to a triple-well potential. This condition enhances the energy harvesting efficiency of wideband vibrations. Measurements were performed on a MEMS e-VEH with a band-limited colored noise.

INTRODUCTION

Kinetic energy is abundantly available in artificial environments such as industrial manufacturing lines, transportations, bridges and also human motions. The technology for harvesting this vibrational power can enable self-sustained, long-lasting and maintenance-free wireless sensors networks [1]. However, mechanical vibrations from natural and artificial sources are mostly inconsistent in time, spread in frequency and located below few hundreds of hertz [2]. Common vibrational energy harvesters (VEHs) are based on spring–mass–damper oscillators and must operate at resonance to maximize the output power. In recent years, some alternative concepts have been proposed to improve the frequency bandwidth: self-tuning resonators [3], piezoelectric cantilever arrays [4] and mechanical frequency-up conversion systems [5]. In addition, the use of nonlinear mechanical oscillators with bi-stable potential was first proposed by Cottone et al. [6] for enhancing the efficiency when harvesting kinetic energy from stochastic vibrations. In that device the bistability was obtained through the force applied to the tip of a cantilever piezoelectric beam by means of opposing magnets. Other bistable solutions based on angular springs [7] or pre-stress buckled beams [8-10] have been shown to increase the output power under both harmonic excitation and band-limited noise.

Among the above solutions, the adoption of nonlinear Duffing-like oscillators has been demonstrated to provide the best choice for developing wideband VEHs in comparison to resonant systems of equal size [11, 12]. This finding is also mostly independent from the conversion technique.

In this paper we show that the MEMS electrostatic VEH, previously presented in [13, 14], provides a tunable multi-stable 3-well potential energy and how this feature can be exploited for an efficient broadband energy harvesting from stochastic vibrations. The impact of nonlinearities for system efficiency is investigated under frequency sweeping and band-limited noise.

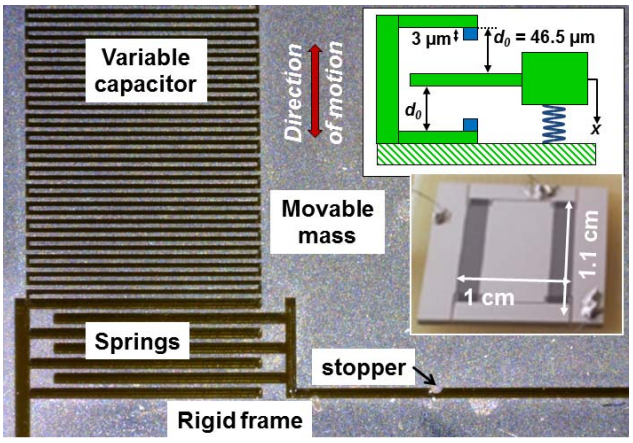

Figure 1: Photographs of the MEMS e-VEH. A schematic of the system model is shown in the upper-right inset.

DESCRIPTION OF THE MEMS

Pictures of the MEMS e-VEH are shown in fig. 1. This device, previously presented in [14], consists of a gap-closing interdigited-comb variable capacitor etched by DRIE (Bosh process) on a 380 µm-thick doped Silicon wafer using an aluminum hard mask layer. The silicon layer is anodically bonded on a glass substrate etched by liquid HF below the moving part. The overall die measures about 10×10 mm^2 of total area. The fingers have a length of 2 mm, width of 30 µm and are separated by a gap of 40.5 µm. The inertial mass of the e-VEH is about 66×10^{-6} kg and is suspended by 4 linear serpentine springs anchored to the rigid frame. Mechanical stoppers allow a minimum gap of 4.5 µm between the movable and fixed fingers of the comb capacitor, so preventing from short circuit when the mass impacts to the rigid frame. Its mechanical resonance results to be of 162 Hz at atmospheric pressure.

MODELING

The gap-closing e-VEH is modeled as a 1-DOF inertial spring-mass-damper oscillator in which the transduction is carried out by the electrical force that arises from the time variation of the capacitance $C(t)$ at constant voltage U_0 [15, 16]. The governing equations of the lumped parameters model are the following:

$$m\frac{d^2x}{dt^2}+(c_a+c_i)\frac{dx}{dt}+\frac{dE_p(x)}{dx}=-m\frac{d^2y}{dt^2}, \quad (1)$$

$$R_L\frac{d}{dt}(C\cdot V)+V=U_0, \quad (2)$$

where the first equation accounts for the mechanical part and the second one for the electrical branch coupled to the system. y and x are the rigid frame and relative displacement of the mass respectively, c_a and c_i are the viscous damping factors in the travelling range before and during the impact with stoppers respectively, V is the instantaneous voltage across the resistive load R_L which is directly connected to the transducer's terminals.

Potential energy

The total potential energy of the system E_p is given by the summation of the mechanical and electrical energy as follows:

$$E_p(x)=\begin{cases}\frac{1}{2}k_{sp}x^2-\frac{1}{2}C(x)U_0^2, & \text{for } |x|<x_{\lim}\\ \frac{1}{2}(k_{sp}+k_{st})x^2-\frac{1}{2}C(x)U_0^2, & \text{for } |x|\geq x_{\lim}\end{cases} \quad (3)$$

where the displacement beyond the stoppers limit x_{lim} is considered in the second part of the piecewise function. k_{st} is the stiffness of the mechanical stoppers calculated as in [17], while k_{sp} is the stiffness of the silicon springs. The variable capacitance $C(x)$ is given by:

$$C(x)=C_{par}+\varepsilon N_f l_f\frac{1}{2r}\left[\ln\left(\frac{d_0-x+2hr}{d_0-x}\right)+\ln\left(\frac{d_0+x+2hr}{d_0+x}\right)\right], \quad (4)$$

where C_{par} is the parasitic capacitance, ε is the air dielectric permittivity, N_f, l_f and h are the number, length and thickness of the comb fingers; $r=tan(\alpha)$ is the aspect ratio related to the sidewalls angle α of the trapezoidal electrodes [14]. In case of perfectly straight sidewalls the capacitance becomes:

$$C_{straight}(x)=\lim_{r\to 0}C(x,r)=\varepsilon N_f l_f\frac{2d_0h}{d_0^2-x^2}. \quad (5)$$

Fig. 2 represents the total potential energy calculated for $|x|<x_{lim}$, for the MEMS device with parameters listed in Table 1, with various U_0 versus mass position. When the electrical force is smaller than the elastic restoring force, the system has only one stable position at $x=0$. When U_0 increases, the potential function tends to flatten, two relative maxima appear in correspondence of the pull-in unstable positions x_{pi} given by:

$$x_{pi}=\pm\left\{d_0^2+2d_0hr+2h^2r^2-\left[2h(d_0+hr)\times\left(2d_0hr^2+2h^2r^3+N_f l_f\varepsilon U_0^2/k_{sp}\right)\right]^{1/2}\right\}^{1/2}. \quad (6)$$

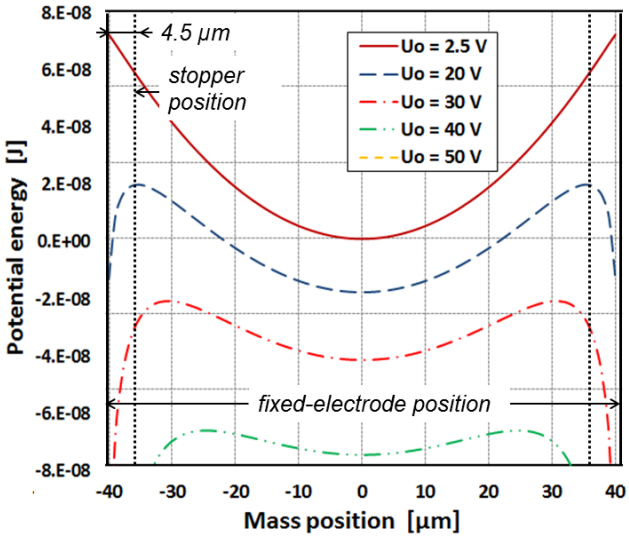

Figure 2: Potential energy of the e-VEH with respect to the mass position.

Beyond these points, two symmetric wells sit on both sides where the mass can remain stuck if the external acceleration is not high enough. The stoppers provide boundaries to the potential energy in order to avoid short circuit and too high pull-in force. On the fig. 2, one can see that these boundaries are close to the unstable equilibrium positions of the mass for low voltage e.g. U_0 ~ 20-30 V. Around U_0 = 20 V the system changes from monostable to multistable behaviour as observed in fig. 2.

The inter-wells jump phenomenon occurs across the pull-in positions x_{pi} for large displacements. Although such an effect has been proven to be advantageous to increase the bandwidth of VEHs [6], it has not yet been investigated for electrostatic gap-closing generators. Similarly to [6, 18], for a certain level of acceleration, an optimal value of the potential barrier height ΔE_p can be found in order to maximize the harvested power. The great advantage of this device is that, such a barrier is tunable through the bias voltage U_0.

Table 1: Model parameters of the e-VEH.

Parameters	**Value/Unit**
Proof mass, m_0	66 mg
Elastic spring stiffness, k_{sp}	68 N m^{-1}
Mechanical resonance, f_r	162 Hz
Active area, A_0	10 × 10 mm^2
Gap between fingers, g_0	40.5 µm
Load resistance, R_L	5.4 MΩ
Device thickness, h	380 µm
Fingers length, l_f	2 mm
Fingers width, w_f	30 µm
Fingers number, N_f	142
Aspect ratio of sidewalls, r	0.013

EXPERIMENTS

Frequency sweeping

Fig. 3 shows the experimental measurements of the output power of the e-VEH for harmonic excitation of $0.25 g_{peak}$. For such a low acceleration, there is no contact of the mobile mass with the stoppers. A typical non-linear behavior due to electrostatic spring softening is observed. When U_0 increases, the flattening of the multistable potential allows a larger displacement of the seismic mass, thus increasing the capacitance ratio C_{max}/C_{min}. With a pre-charge U_0 up to 30V, the frequency sweep-up and sweep-down curves are identical. But beyond 30 V, an hysteresis appears. This is a typical behavior of a multistable VEH like in [6-8]. This effect is due to the presence of multiple harmonic solutions which is common for Duffing-like oscillators. At 50 V, an unstable behavior starts to be observed, and for higher voltages, the electrostatic instability (pull-in) is reached and the mobile electrode sticks on the fixed one.

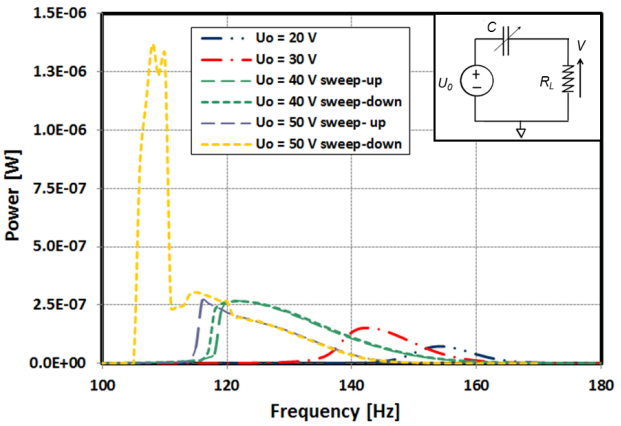

Figure 3: Harvested power on a 5.4 MΩ load for a sweeping sinusoidal vibration of 0.25 g in amplitude

Stochastic excitation

Fig. 5 shows the response of the e-VEH excited under stochastic vibrations. In particular, a low−frequency exponentially correlated noise with autocorrelation time of 0.01 *s* was used. The corresponding frequency band is limited by a cut-off frequency around 160 Hz. A first test was carried out with an acceleration level of 0.25 g_{rms} with different values of U_0. The power spectral density PSD of the generated input vibration is shown in fig. 4. The useful bandwidth for the harvested power increases significantly for $U_0 \geq 30$V. For $U_0 = 50$V, the harvested power is more than an order of magnitude higher than at lower U_0 for frequencies between 50 to 100 Hz and above 150 Hz.

Fig.6 illustrates experimental tests repeated with an acceleration level of 1 g_{rms} for different values of U_0. We would expect that for an increasing acceleration the harvested power would be highest at maximum pre-charge voltage as for the previous case of 0.25 g_{rms}. On the contrary, at 1 g_{rms} the maximum power and bandwidth are obtained for $U_0 = 40$ V while the harvested power decreases drastically for $U_0 = 50$ V. A possible interpretation of this effect is the following: if the acceleration is too high, the systems does not get

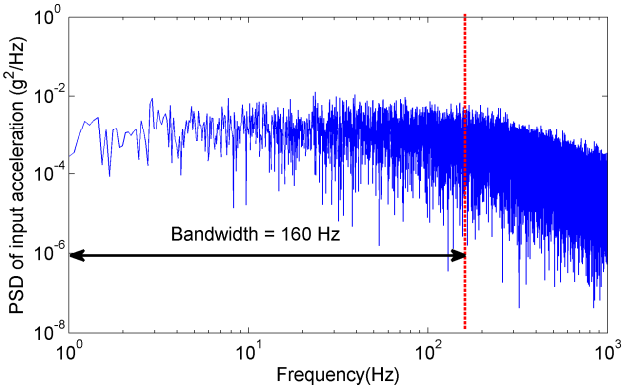

Figure 4: Input excitation PSD of band-limited colored noise with acceleration level of 1 g_{rms}. A similar PSD was used for 0.25 g_{rms}.

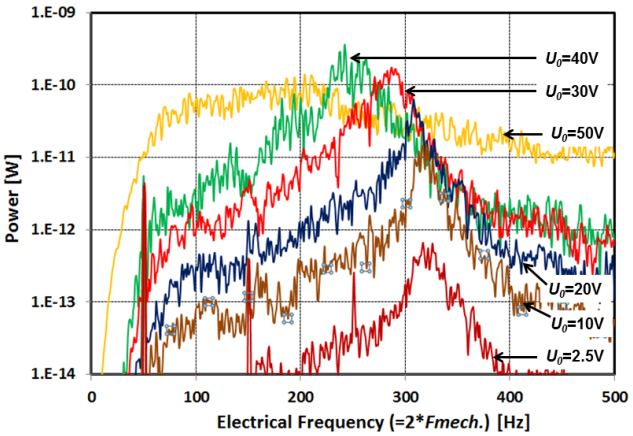

Figure 5: Harvested power on a 5.4 MΩ load for a similar input noise that in fig. 4 but with an acceleration level of 0.25 g_{rms}

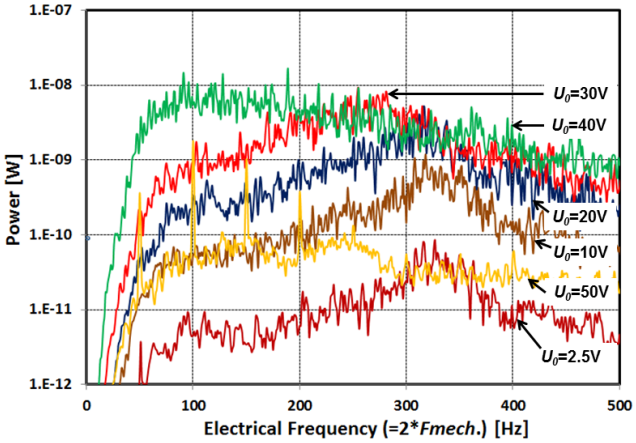

Figure 6: Harvested power on a 5.4 MΩ load for the input noise in fig. 4 (acceleration level of 1 g_{rms}).

advantage by the multistable shape of the potential energy in terms of inter-well and intra-well oscillations but frequently hits the mechanical stoppers. As a consequence it damps more kinetic energy during impacts and sticks to the boundaries. Therefore, at each acceleration level there exists an optimal value of pre-charge voltage U_0, hence of the energy barriers of the potential energy, that must be

found in order to maximize the harvested power.

CONCLUSION

An electrostatic vibration energy harvester based on silicon MEMS gap-closing combs was investigated under harmonic and stochastic vibrations. The device features a multi-stable 3-well potential energy that can be tuned by changing the pre-charge voltage U_0 of the capacitor. This characteristic is demonstrated to be beneficial to enlarge the frequency bandwidth of the system and improve the harvested power.

Under frequency sweeping at $0.25\,g$, a typical electrostatic spring softening is observed and for U_0 beyond 30 V an hysteresis between up and down sweeps occurs. Under band-limited noise at 0.25 g_{rms} the system bandwidth significantly widens from $U_0 = 30$V, whereas an order of magnitude more power is harvested at lower frequencies between 50 to 100 Hz and above 150 Hz for $U_0 = 50$V. Contrary to the expectations, at 1 g_{rms}, the optimal voltage resulted to be of $U_0 = 40$ V. This suggests that the nonlinear potential energy must be tuned to the specific acceleration level in order to get advantage from multistability.

ACKNOWLEDGEMENTS

The authors gratefully acknowledge the support of FP7 Marie Curie IEF funding scheme (NEHSTech, Grant N. 275437) at Université de Paris-Est, ESIEE Paris and French National Research Agency through the contract ANR-08-SEGI-019.

REFERENCES:

[1] M. Kroener, "Energy harvesting technologies: Energy sources, generators and management for wireless autonomous applications," 2012, pp. 1-4.

[2] S. Roundy, *et al.*, *Energy Scavenging For Wireless Sensor Networks with special focus on Vibrations*: Kluwer Academic Publisher, 2004.

[3] D. Zhu, *et al.*, "Design and experimental characterization of a tunable vibration-based electromagnetic micro-generator," *Sensors and Actuators A: Physical,* vol. 158, pp. 284-293, 2010.

[4] M. Ferrari, *et al.*, "Improved energy harvesting from wideband vibrations by nonlinear piezoelectric converters," *Sensors and Actuators A: Physical,* 2010.

[5] S. M. Jung and K. S. Yun, "Energy-harvesting device with mechanical frequency-up conversion mechanism for increased power efficiency and wideband operation," *Applied Physics Letters,* vol. 96, p. 111906, 2010.

[6] F. Cottone, *et al.*, "Nonlinear energy harvesting," *Physical Review Letters,* vol. 102, 2009.

[7] S. D. Nguyen, *et al.*, "Bistable springs for wideband microelectromechanical energy harvesters," *Applied Physics Letters,* vol. 102, pp. 023904-023904-4, 2013.

[8] F. Cottone, *et al.*, "Piezoelectric buckled beams for random vibration energy harvesting," *Smart materials and structures,* vol. 21, 2012.

[9] R. Masana and M. Daqaq, "Energy harvesting in the super-harmonic frequency region of a twin-well oscillator," *Journal of Applied Physics,* vol. 111, pp. 044501-044501-11, 2012.

[10] W. Liu, *et al.*, "Novel piezoelectric bistable oscillator architecture for wideband vibration energy harvesting," *Smart materials and structures,* vol. 22, p. 035013, 2013.

[11] R. Harne and K. Wang, "A review of the recent research on vibration energy harvesting via bistable systems," *Smart materials and structures,* vol. 22, p. 023001, 2013.

[12] D. Hoffmann, *et al.*, "Comparative study of concepts for increasing the bandwidth of vibration based energy harvesters," in *PowerMEMS*, Atlanta, GA, USA, 2012, pp. 219-220.

[13] F. Cottone, *et al.*, "Bistable multiple-mass electrostatic generator for low-frequency vibration energy harvesting," in *IEEE 26th Int. Conf. on MEMS*, Taipei, 2013.

[14] R. Guillemet, *et al.*, "Wideband MEMS electrostatic vibration energy harvesters based on gap-closing interdigited combs with a trapezoidal section," in *IEEE 26th Int. Conf. on MEMS*, Taipei, 2013.

[15] P. Basset, *et al.*, "A batch-fabricated and electret-free silicon electrostatic vibration energy harvester," *Journal of Micromechanics and Microengineering,* vol. 19, p. 115025, 2009.

[16] G. Despesse, *et al.*, "Fabrication and characterisation of high damping electrostatic micro devices for vibration energy scavenging," *Proc. Design, Test, Integration and Packaging of MEMS and MOEMS,* pp. 386–90, 2005.

[17] C. P. Le and E. Halvorsen, "MEMS electrostatic energy harvesters with end-stop effects," *Journal of Micromechanics and Microengineering,* vol. 22, p. 074013, 2012.

[18] L. Gammaitoni, *et al.*, "Nonlinear oscillators for vibration energy harvesting," *Applied Physics Letters,* vol. 94, pp. 164102-164102-3, 2009.

CONTACT

*F. Cottone, f.cottone@esiee.fr.